

Preassembly Strategy To Fabricate Porous Hollow Carbonitride Spheres Inlaid with Single Cu–N₃ Sites for Selective Oxidation of Benzene to Phenol

Ting Zhang,[†] Di Zhang,[†] Xinghua Han,[‡] Ting Dong,[‡] Xinwen Guo,^{†,§} Chunshan Song,^{†,||} Rui Si,^{*,§} Wei Liu,[#] Yuefeng Liu,^{*,#} and Zhongkui Zhao^{*,†}

[†]State Key Laboratory of Fine Chemicals, PSU-DUT Joint Center for Energy Research, School of Chemical Engineering, Dalian University of Technology, Dalian 116024, P. R. China

[‡]School of Chemical Engineering and Technology, North University of China, Taiyuan 030051, P. R. China

^{||}EMS Energy Institute, PSU-DUT Joint Center for Energy Research and Department of Energy & Mineral Engineering and Chemical Engineering, Pennsylvania State University, University Park, Pennsylvania 16802, United States

[§]Shanghai Synchrotron Radiation Facility, Shanghai Institute of Applied Physics, Chinese Academy of Sciences, Shanghai 201204, P.R. China

[#]Dalian National Laboratory for Clean Energy, Dalian Institute of Chemical Physics, Chinese Academy of Sciences, Dalian 116023, P. R. China

Supporting Information

ABSTRACT: Developing single-atom catalysts with porous micro-/nanostructures for high active-site accessibility is of great significance but still remains a challenge. Herein, we for the first time report a novel template-free preassembly strategy to fabricate porous hollow graphitic carbonitride spheres with single Cu atoms mounted via thermal polymerization of supramolecular preassemblies composed of a melamine–Cu complex and cyanuric acid. Atomically dispersed Cu–N₃ moieties were unambiguously confirmed by spherical aberration correction electron microscopy and extended X-ray absorption fine structure spectroscopy. More importantly, this material exhibits outstanding catalytic performance for selective oxidation of benzene to phenol at room temperature, especially showing phenol selectivity (90.6 vs 64.2%) and stability much higher than those of the supported Cu nanoparticles alone, originating from the isolated unique Cu–N₃ sites in the porous hollow structure. An 86% conversion of benzene, with an unexpectedly high phenol selectivity of 96.7% at 60 °C for 12 h, has been achieved, suggesting a great potential for practical applications. This work paves a new way to fabricate a variety of single-atom catalysts with diverse graphitic carbonitride architectures.

Phenol, an industrially important chemical, has been mostly produced from benzene by a three-step cumene process in industry, which leads to heavy environmental pollution.¹ Direct oxidation of benzene to phenol with clean oxidants, such as oxygen or H₂O₂, is considered an ideal process.² In this regard, graphitic carbon nitride (g-C₃N₄), also called graphitic carbonitride, was found to be active as a metal-free catalyst for selective oxidation of benzene to phenol under mild conditions.³ However, it meets the barrier of low catalytic activity.⁴ Iron-doped carbon nitride showed improved activity,

yet still unsatisfactory.^{3,5} Owing to their unique electronic properties, remarkably promoted catalytic properties, and high atom utilization, single-atom catalysts (SACs) have attracted great interest.^{6–11} Combination of Fe-SACs and N-doped carbon materials notably enhanced the activity of benzene oxidation to phenol, thus opening a new field for investigation.^{12,13} Furthermore, copper-based materials have been generally considered to be efficient selective oxidation catalysts.^{14–16} Considering the abundant N content and chemical stability of g-C₃N₄,¹⁷ and the fact that N atoms provide anchoring sites for stabilizing metal atoms, Cu-SACs/g-C₃N₄ composites are expected to be more efficient for selective oxidation of benzene to phenol.

Thermal condensation is a promising approach to prepare SACs. However, embedding metal atoms inside bulk support suffers from a disadvantage regarding the depressed accessibility of active sites to reactants.^{18,19} To deposit single metal atoms on the surface of various supports is considered as an alternative to improve the accessibility of SACs,^{20–26} yet materials formed in this way still suffer from the barrier of an extremely low metal loading. Further increasing the accessibility but with a relatively higher loading remains an interesting issue. SACs with unique morphologies prepared by pyrolysis using hard templates showed improved accessibility.^{27–31} However, the hard-template method is hindered by a complex preparation process, active metal leaching, and high cost in the essential de-templating process, such as hydrothermal alkali/acid treatment or high-temperature vaporization. Especially for the heating acid treatment, choosing an inappropriate leaching solution would result in significant loss of active metals.^{32,33} In spite of extensive efforts, the search for a facile, template-free approach for preparing single metallic atoms mounted in nano-/microstructures is still challenging. It was previously

Received: October 15, 2018

Published: November 30, 2018



reported that different $g\text{-C}_3\text{N}_4$ nano-/microstructures were successfully prepared by forming preorganized supramolecules.³⁴ Therefore, we envision that single atoms can be implanted in $g\text{-C}_3\text{N}_4$ nano-/microstructures by a template-free preassembly method using a metal complex as a building block for supramolecular assembly, but it remains unconfirmed.

Herein, we put forward, for the first time, a novel template-free preassembly strategy to fabricate porous hollow $g\text{-C}_3\text{N}_4$ spheres (HCNS) inlaid with single Cu atoms through thermal polymerization of Cu-containing supramolecular assemblies formed by the preassembly of a melamine–Cu complex with cyanuric acid (Scheme 1), generating a new and efficient

Scheme 1. Illustration of the Synthesis of Cu-SA/HCNS



single-atom Cu catalyst (denoted as Cu-SA/HCNS) for selective oxidation of benzene to phenol. Typically, copper nitrate, as the Cu source, was first complexed with melamine to produce a melamine–Cu complex in DMSO. The cyanuric acid-dissolved DMSO was then decanted slowly into the above solution under stirring. The resulting white precipitate was washed with deionized water and then ethanol, followed by thermal polymerization under a N_2 atmosphere at $550\text{ }^\circ\text{C}$ to form Cu-SA/HCNS directly. Thanks to both atomically dispersed Cu– N_3 species and promoted accessibility by the porous hollow structure, Cu-SA/HCNS exhibits outstanding catalytic performance in the selective oxidation of benzene to phenol, especially showing phenol selectivity much higher than that observed with the supported Cu nanoparticles alone at room temperature. Importantly, a high benzene conversion of 86%, with an unexpectedly high phenol selectivity of 96.7% at $60\text{ }^\circ\text{C}$ for 12 h, is achieved, indicating a great potential for practical application. This work not only presents a novel and highly efficient catalyst for selective oxidation of benzene to phenol but also paves a new way for designing and fabricating diverse single-atom catalysts in different graphitic carbonitride nano-/microarchitectures for use in other transformations.

Scanning electron microscopy (SEM) and transmission electron microscopy (TEM) images (Figure 1a,b) reveal that the Cu-SA/HCNS catalyst features a regular hollow spherical structure with ca. 3 nm pores (Figure S1). A high-resolution (HR) TEM image indicates no nanoparticles or clusters to be observed on Cu-SA/HCNS (Figure 1c). The single Cu atoms are identified as bright spots (highlighted by yellow circles) by high-angle annular dark-field scanning transmission electron microscopy (HAADF-STEM) (Figure 1d). Figure 1e shows two characteristic X-ray diffraction (XRD) peaks appearing at 27.4° and 13.0° , assigned to $g\text{-C}_3\text{N}_4$, with decreasing intensity for Cu-SA/HCNS in contrast to bare HCNS, indicating that the insertion of a Cu atom distorts the crystal structure of $g\text{-C}_3\text{N}_4$. It should be noted that, although Cu-SA/HCNS shows a lowering crystallinity, the morphology and main matrix of $g\text{-C}_3\text{N}_4$ are not largely influenced. From elemental analysis results, Cu-SA/HCNS shows a N/C ratio similar to that of HCNS (ca. 1.5, Table S1), presenting further evidence for no obvious change in the carbonitride matrix after the introduction of Cu atoms. From N_2 adsorption–desorption measurements, Cu-SA/HCNS has a higher specific surface area

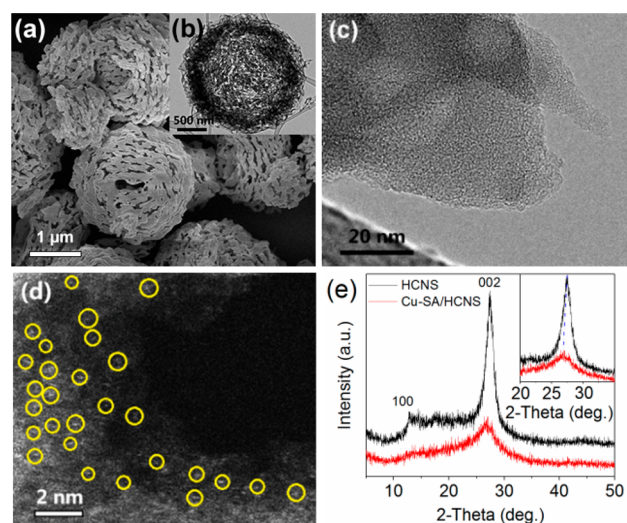


Figure 1. (a) SEM, (b) TEM, (c) HRTEM, and (d) HAADF-STEM images of Cu-SA/HCNS. (e) XRD patterns of HCNS matrix and Cu-SA/HCNS.

and Barrett–Joyner–Halenda pore volume than bare HCNS (Figure S1), possibly resulting from the replacement of melamine by melamine–Cu complex in the supramolecular aggregates. The XRD peak of HCNS at 27.4° assigned to interlayer stacking of the conjugated aromatic systems shifts to 26.8° for Cu-SA/HCNS (inset in Figure 1e), indicating an increased carbonitride interlayer distance. Thus, the loose carbonitride structure was obtained (Figure S2). The porous hollow loose structure promotes accessibility of single Cu atoms to reactants, subsequently endowing Cu-SA/HCNS with promoted catalytic performance.

Coordination-unsaturated sites like in-plane N atoms in $g\text{-C}_3\text{N}_4$ are easily formed during thermal polymerization,^{35–37} which is crucial to forming isolated Cu atoms in HCNS. The X-ray photoelectron spectroscopy (XPS) peak of Cu-SA/HCNS attributed to pyridinic N shows a shift to a lower bonding energy value compared to that of HCNS alone (Figure S3a,b), suggesting that Cu atoms coordinate with pyridinic N to form the Cu– N_x moieties.^{38,39} The melamine–Cu complex (marked as $\text{Cu}(\text{NO}_3)_2(\text{Mel})$) was prepared in DMSO solvent. The weakened strength of the triazine ring vibration and red-shift of side-chain C–N stretching confirm the formation of the $\text{Cu}(\text{NO}_3)_2(\text{Mel})$ complex via a Cu–N bond (Figure S4).⁴⁰ N 1s XPS spectra (Figure 2a,b) further feature a new bond (399.0 eV), indicating the formation of a Cu–N bond.³⁰ The N atoms in the $\text{Cu}(\text{NO}_3)_2(\text{Mel})$ complex strongly coordinate with the Cu atoms. Meanwhile, N atoms from cyanuric acid may also stabilize Cu atoms in the thermal polymerization process, resulting in a uniform distribution of isolated Cu atoms in Cu-SA/HCNS.⁴¹ The Cu content determined by inductively coupled plasma–atomic emission spectroscopy analysis is ca. 0.85 wt%. Although the Cu 2p XPS spectrum of fresh Cu-SA/HCNS shows no peak attributable to surface Cu species, a peak at 932.3 eV, assigned to Cu^+ , emerges after 60 s of etching (Figure S3c). The surface Cu contents before and after etching are 0.33 and 0.64 atom%, respectively (Table S2), indicating well-distributed Cu atoms in the HCNS matrix.

To explore the electronic structure and coordination environment of Cu species in Cu-SA/HCNS, we conducted X-ray absorption fine structure (XAFS) measurements. X-ray

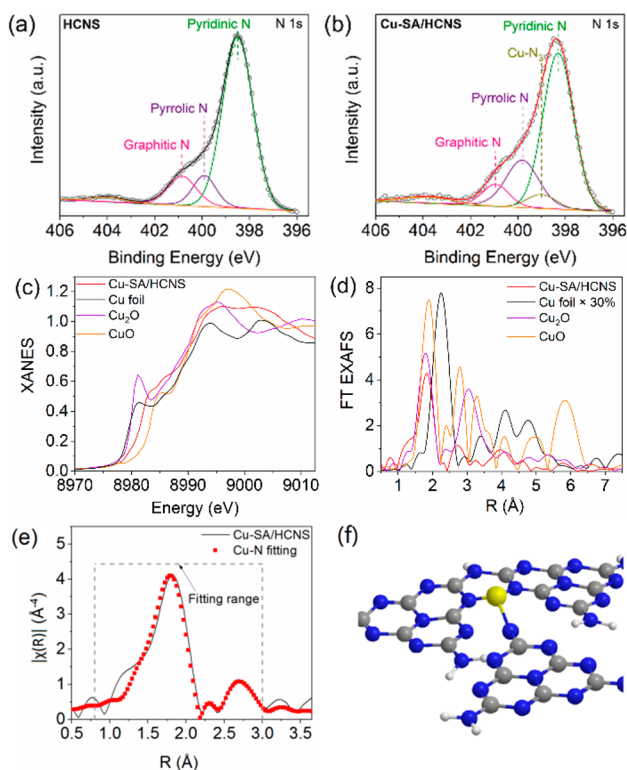


Figure 2. (a,b) N 1s XPS spectra of Cu-SA/HCNS and bare HCNS. (c) Normalized Cu K-edge XANES spectra of Cu foil, CuO, Cu₂O, and Cu-SA/HCNS. (d) k^3 -weighted Fourier transform spectra from Cu K-edge EXAFS. (e) The corresponding EXAFS fitting curve of Cu-SA/HCNS. (f) Model of Cu–N₃ sites in Cu-SA/HCNS: Cu (yellow), C (gray), N (blue), and H (white).

absorption near-edge spectroscopy (XANES) of fresh Cu-SA/HCNS reveals similar edge shapes for both Cu₂O and CuO references (Figure 2c), identifying the oxidized Cu^{δ+} ($1 < \delta < 2$) state. The corresponding linear combination fits⁴² provide the average valence of Cu as +1.6, revealing the higher oxidized state of single Cu atoms. The related extended X-ray absorption fine structure (EXAFS) spectrum in R space for Cu-SA/HCNS is significantly different from the spectra of the bulk references of Cu foil, Cu₂O, and CuO (Figure 2d). No obvious Cu–Cu interaction can be detected, indicating that Cu atoms are atomically dispersed in the HCNS matrix. The related fitting curves in Figure 2e exhibit a prominent peak at 1.9–2.0 Å derived from the first shell of Cu–N (Table S3) plus a weak contribution at 2.8–2.9 Å originating from replacement of the second shell of Cu–N or Cu–C in the C₃N₄ model by a Cu center. Furthermore, Table S3 shows that the coordination number (CN) of the fitted first shell (Cu–N: 3.3 ± 0.3) is significantly higher than that of the second shell (Cu–N/C: 1.7 ± 0.4), indicating a large degree of disorder for the coordination structure around the copper single atoms, which is in agreement with the former XRD results. Therefore, the isolated Cu atomic structure is modeled by density functional theory, and as described in Figure 2f, the Cu atom is coordinated by three N atoms.

C–H bond activation is of great importance for transformation.^{43,44} Herein, the catalytic performance of Cu-SA/HCNS for C–H activation was first evaluated by employing selective oxidation of benzene to phenol, an industrially important conversion, as a model reaction (Figure 3).

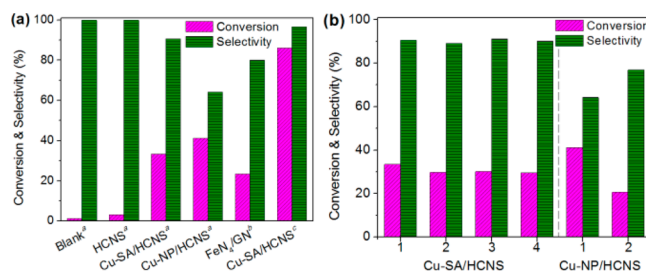


Figure 3. (a) Catalytic performance of diverse materials. ^a25 °C and 24 h; ^bRef 3, 60 °C and 24 h; ^c60 °C and 12 h. (b) Recyclability of the Cu-SA/HCNS and Cu-NP/HCNS catalysts.

The supported Cu nanoparticle catalyst on HCNS (Cu-NP/HCNS, TEM images shown in Figure S5) was tested as a benchmark for comparison (Figure 3a). Only a trace amount of benzene is converted if the reaction is performed in the absence of catalyst (blank experiment) or over the bare HCNS support. Cu-SA/HCNS catalyst shows a benzene conversion of 33.4%, with a phenol selectivity of 90.6% at 25 °C for 24 h. Furthermore, 86.0% benzene conversion is achieved with high phenol selectivity of 96.7% at 60 °C for 12 h over Cu-SA/HCNS. Cu-SA/HCNS shows much superior catalytic properties compared to the previously reported SACs (Table S4),^{12,13} ascribed to the atomically dispersed unique Cu–N₃ species and the efficiently promoted accessibility of active sites by the porous hollow structure. More interestingly, Cu-SA/HCNS shows much higher phenol selectivity than the supported Cu NPs, although the single Fe sites did not indicate higher selectivity than Fe NPs.^{12,13} From kinetic studies (Figures S6 and S7 and Table S5), the much higher selectivity of Cu-SA/HCNS compared to Cu-NP/HCNS originates from the efficient inhibition of deep oxidation by the much higher apparent activation barrier and much lower pre-exponential factor, owing to the unique Cu–N₃ sites. Recyclability of both Cu-SA/HCNS and Cu-NP/HCNS is checked (Figure 3b). No obviously decrease in benzene conversion and phenol selectivity over Cu-SA/HCNS catalyst can be observed, while the benzene conversion drops dramatically from 41.2% to 20% for the second run over Cu-NP/HCNS. The reaction and characterization results demonstrate that the single Cu atoms in HCNS are stabilized during the reaction owing to the strongly anchored Cu–N₃ species in the HCNS matrix (Figures 3b and S8, and Table S6).

In conclusion, we present a novel and facile preassembly strategy to prepare a porous hollow spherical g-C₃N₄ catalyst inlaid with single Cu atoms with unique Cu–N₃ species and high accessibility of active sites. Interestingly, the developed Cu-SA/HCNS catalyst exhibits excellent catalytic performance, particularly much higher phenol selectivity and stability for selective oxidation of benzene to phenol, in comparison with the supported Cu nanoparticles. The anchored, atomically dispersed unique Cu–N₃ species are responsible for the outstanding catalytic behavior. This work not only provides a novel and efficient catalyst for selective oxidation of benzene to phenol but also paves a new avenue to design and fabricate a variety of single-atom catalysts in g-C₃N₄ micro/nano-architectures by changing metals and/or tuning the structures of the preorganized supramolecular aggregates for diverse transformations.

■ ASSOCIATED CONTENT

● Supporting Information

The Supporting Information is available free of charge on the ACS Publications website at DOI: 10.1021/jacs.8b10703.

Detailed experimental procedures, characterization methods, and additional data, including Figures S1–S8 and Tables S1–S6 (PDF)

■ AUTHOR INFORMATION

Corresponding Authors

*sirui@sinap.ac.cn

*yuefeng.liu@dicp.ac.cn

*zkzhao@dlut.edu.cn

ORCID 

Xinwen Guo: 0000-0002-6597-4979

Chunshan Song: 0000-0003-2344-9911

Yuefeng Liu: 0000-0001-9823-3811

Zhongkui Zhao: 0000-0001-6529-5020

Notes

The authors declare no competing financial interest.

■ ACKNOWLEDGMENTS

This work was financially supported by National Natural Science Foundation of China (U1610104 and 21676046).

■ REFERENCES

- (1) Wang, Y.; Wang, X.; Antonietti, M. Polymeric Graphitic Carbon Nitride as a Heterogeneous Organocatalyst: From Photochemistry to Multipurpose Catalysis to Sustainable Chemistry. *Angew. Chem., Int. Ed.* **2012**, *51*, 68–89.
- (2) Bal, R.; Tada, M.; Sasaki, T.; Iwasawa, Y. Direct Phenol Synthesis by Selective Oxidation of Benzene with Molecular Oxygen on an Interstitial-N/Re Cluster/Zeolite Catalyst. *Angew. Chem., Int. Ed.* **2006**, *45*, 448–452.
- (3) Chen, X.; Zhang, J.; Fu, X.; Antonietti, M.; Wang, X. Fe-g-C₃N₄-Catalyzed Oxidation of Benzene to Phenol Using Hydrogen Peroxide and Visible Light. *J. Am. Chem. Soc.* **2009**, *131*, 11658–11659.
- (4) Wang, Y.; Di, Y.; Antonietti, M.; Li, H.; Chen, X.; Wang, X. Excellent Visible-Light Photocatalysis of Fluorinated Polymeric Carbon Nitride Solids. *Chem. Mater.* **2010**, *22*, 5119–5121.
- (5) Di, Y.; Wang, X.; Thomas, A.; Antonietti, M. Making Metal Carbon Nitride Heterojunctions for Improved Photocatalytic Hydrogen Evolution with Visible Light. *ChemCatChem* **2010**, *2*, 834–838.
- (6) Qiao, B.; Wang, A.; Yang, X.; Allard, L. F.; Jiang, Z.; Cui, Y.; Liu, J.; Li, J.; Zhang, T. Single-atom catalysis of CO oxidation using Pt₁/FeO_x. *Nat. Chem.* **2011**, *3*, 634–641.
- (7) Mitchell, S.; Vorobyeva, E.; Pérez-Ramírez, J. The Multifaceted Reactivity of Single-Atom Heterogeneous Catalysts. *Angew. Chem., Int. Ed.* **2018**, *57*, 15316.
- (8) Rogge, S. M. J.; Bavykina, A.; Hajek, J.; Garcia, H.; Olivos-Suarez, A. I.; Sepúlveda-Escribano, A.; Vimont, A.; Clet, G.; Bazin, P.; Kapteijn, F.; Daturi, M.; Ramos-Fernandez, E. V.; Llabrés Xamena, F. X.; Van Speybroeck, V.; Gascon, J. Metal–organic and covalent organic frameworks as single-site catalysts. *Chem. Soc. Rev.* **2017**, *46*, 3134–3184.
- (9) Yamashita, H.; Mori, K.; Kuwahara, Y.; Kamegawa, T.; Wen, M.; Verma, P.; Che, M. Single-site and nano-confined photocatalysts designed in porous materials for environmental uses and solar fuels. *Chem. Soc. Rev.* **2018**, *47*, 8072–8096.
- (10) Chen, Y.; Ji, S.; Chen, C.; Peng, Q.; Wang, D.; Li, Y. Single-Atom Catalysts: Synthetic Strategies and Electrochemical Applications. *Joule* **2018**, *2*, 1242–1264.

(11) Risse, T.; Shaikhutdinov, S.; Nilius, N.; Sterrer, M.; Freund, H. Gold Supported on Thin Oxide Films: From Single Atoms to Nanoparticles. *Acc. Chem. Res.* **2008**, *41*, 949–956.

(12) Zhang, M.; Wang, Y.; Chen, W.; Dong, J.; Zheng, L.; Luo, J.; Wan, J.; Tian, S.; Cheong, W.; Wang, D.; Li, Y. Metal (Hydr)oxides@ Polymer Core-Shell Strategy to Metal Single Atom Materials. *J. Am. Chem. Soc.* **2017**, *139*, 10976–10979.

(13) Deng, D.; Chen, X.; Yu, L.; Wu, X.; Liu, Q.; Liu, Y.; Yang, H.; Tian, H.; Hu, Y.; Du, P.; Si, R.; Wang, J.; Cui, X.; Li, H.; Xiao, J.; Xu, T.; Deng, J.; Yang, F.; Duchesne, P. N.; Zhang, P.; Zhou, J.; Sun, L.; Li, J.; Pan, X.; Bao, X. A single iron site confined in a grapheme matrix for the catalytic oxidation of benzene at room temperature. *Sci. Adv.* **2015**, *1*, No. e1500462.

(14) Tomkins, P.; Ranocchiari, M.; van Bokhoven, J. A. Direct Conversion of Methane to Methanol under Mild Conditions over Cu-Zeolites and beyond. *Acc. Chem. Res.* **2017**, *50*, 418–425.

(15) Ikuno, T.; Zheng, J.; Vjunov, A.; Sanchez-Sanchez, M.; Ortuño, M. A.; Pahls, D. R.; Fulton, J. L.; Camaioni, D. M.; Li, Z.; Ray, D.; Mehdi, B. L.; Browning, N. D.; Farha, O. K.; Hupp, J. T.; Cramer, C. J.; Gagliardi, L.; Lercher, J. A. Methane Oxidation to Methanol Catalyzed by Cu-Oxo Clusters Stabilized in NU-1000 Metal–Organic Framework. *J. Am. Chem. Soc.* **2017**, *139*, 10294–10301.

(16) Yamaguchi, S.; Suzuki, A.; Togawa, M.; Nishibori, M.; Yahiro, H. Selective Oxidation of Thioanisole with Hydrogen Peroxide using Copper Complexes Encapsulated in Zeolite: Formation of a Thermally Stable and Reactive Copper Hydroperoxo Species. *ACS Catal.* **2018**, *8*, 2645–2650.

(17) Zhao, Z.; Ge, G.; Zhang, D. Heteroatom-Doped Carbonaceous Photocatalysts for Solar Fuel Production and Environmental Remediation. *ChemCatChem* **2018**, *10*, 62–123.

(18) Kang, X.; Liu, H.; Hou, M.; Sun, X.; Han, H.; Jiang, T.; Zhang, Z.; Han, B. Synthesis of Supported Ultrafine Non-noble Subnanometer-Scale Metal Particles Derived from Metal–Organic Frameworks as Highly Efficient Heterogeneous Catalysts. *Angew. Chem., Int. Ed.* **2016**, *55*, 1080–1084.

(19) Wang, A.; Li, J.; Zhang, T. Heterogeneous single-atom catalysis. *Nat. Rev. Chem.* **2018**, *2*, 65–81.

(20) Yusoff, A. R. M.; Kim, D.; Schneider, F. K.; da Silva, W. J.; Jang, J. Au-doped single layer graphene nanoribbons for a record-high efficiency ITO-free tandem polymer solar cell. *Energy Environ. Sci.* **2015**, *8*, 1523–1537.

(21) Zhang, D.; Chen, W.; Li, Z.; Chen, Y.; Zheng, L.; Gong, Y.; Li, Q.; Shen, R.; Han, Y.; Cheong, W.; Gu, L.; Li, Y. Isolated Fe and Co dual active sites on nitrogen-doped carbon for a highly efficient oxygen reduction reaction. *Chem. Commun.* **2018**, *54*, 4274–4277.

(22) Lang, R.; Li, T.; Matsumura, D.; Miao, S.; Ren, Y.; Cui, Y.; Tan, Y.; Qiao, B.; Li, L.; Wang, A.; Wang, X.; Zhang, T. Hydroformylation of Olefins by a Rhodium Single-Atom Catalyst with Activity Comparable to RhCl(PPh₃)₃. *Angew. Chem., Int. Ed.* **2016**, *55*, 16054–16058.

(23) Zhang, B.; Asakura, H.; Zhang, J.; Zhang, J.; De, S.; Yan, N. Stabilizing a Platinum₁ Single-Atom Catalyst on Supported Phosphomolybdic Acid without Compromising Hydrogenation Activity. *Angew. Chem., Int. Ed.* **2016**, *55*, 8319–8323.

(24) Wang, L.; Li, H.; Zhang, W.; Zhao, X.; Qiu, J.; Li, A.; Zheng, X.; Hu, Z.; Si, R.; Zeng, J. Supported Rhodium Catalysts for Ammonia–Borane Hydrolysis: Dependence of the Catalytic Activity on the Highest Occupied State of the Single Rhodium Atoms. *Angew. Chem., Int. Ed.* **2017**, *56*, 4712–4718.

(25) Li, X.; Bi, W.; Zhang, L.; Tao, S.; Chu, W.; Zhang, Q.; Luo, Y.; Wu, C.; Xie, Y. Single-Atom Pt as Co-Catalyst for Enhanced Photocatalytic H₂ Evolution. *Adv. Mater.* **2016**, *28*, 2427–2431.

(26) Zhang, J.; Liu, J.; Xi, L.; Yu, Y.; Chen, N.; Sun, S.; Wang, W.; Lange, K. M.; Zhang, B. Single-Atom Au/NiFe Layered Double Hydroxide Electrocatalyst: Probing the Origin of Activity for Oxygen Evolution Reaction. *J. Am. Chem. Soc.* **2018**, *140*, 3876–3879.

(27) Yusoff, A. R. M.; Kim, D.; Schneider, F. K.; da Silva, W. J.; Jang, J. Au-doped single layer graphenenanoribbons for a record-high

efficiency ITO-free tandem polymer solar cell. *Energy Environ. Sci.* **2015**, *8*, 1523–1537.

(28) Han, Y.; Wang, Z.; Xu, R.; Zhang, W.; Chen, W.; Zheng, L.; Zhang, J.; Luo, J.; Wu, K.; Zhu, Y.; Chen, C.; Peng, Q.; Liu, Q.; Hu, P.; Wang, D.; Li, Y. Ordered Porous Nitrogen-Doped Carbon Matrix with Atomically Dispersed Cobalt Sites as an Efficient Catalyst for Dehydrogenation and Transfer Hydrogenation of N-Heterocycles. *Angew. Chem., Int. Ed.* **2018**, *57*, 11262–11266.

(29) Han, Y.; Wang, Y.; Chen, W.; Xu, R.; Zheng, L.; Zhang, J.; Luo, J.; Shen, R.; Zhu, Y.; Cheong, W.; Chen, C.; Peng, Q.; Wang, D.; Li, Y. Hollow N-Doped Carbon Spheres with Isolated Cobalt Single Atomic Sites: Superior Electrocatalysts for Oxygen Reduction. *J. Am. Chem. Soc.* **2017**, *139*, 17269–17272.

(30) Zhang, H.; Wei, J.; Dong, J.; Liu, G.; Shi, L.; An, P.; Zhao, G.; Kong, J.; Wang, X.; Meng, X.; Zhang, J.; Ye, J. Efficient Visible-Light-Driven Carbon Dioxide Reduction by a Single-Atom Implanted Metal–Organic Framework. *Angew. Chem., Int. Ed.* **2016**, *55*, 14310–14314.

(31) Malonzo, C. D.; Shaker, S. M.; Ren, L.; Prinslow, S. D.; Platero-Prats, A. E.; Gallington, L. C.; Borycz, J.; Thompson, A. B.; Wang, T. C.; Farha, O. K.; Myers, J. C.; Penn, R. L.; Gagliardi, L.; Tsapatsis, M.; Stein, A.; et al. Thermal Stabilization of Metal–Organic Framework-Derived Single Site Catalytic Clusters through Nanocasting. *J. Am. Chem. Soc.* **2016**, *138*, 2739–2748.

(32) Liu, W.; Chen, Y.; Qi, H.; Zhang, L.; Yan, W.; Liu, X.; Yang, X.; Miao, S.; Wang, W.; Liu, C.; Wang, A.; Li, J.; Zhang, T. A Durable Nickel Single-Atom Catalyst for Hydrogenation Reactions and Cellulose Valorization under Harsh Conditions. *Angew. Chem., Int. Ed.* **2018**, *57*, 7071–7075.

(33) Liu, W.; Zhang, L.; Liu, X.; Liu, X.; Yang, X.; Miao, S.; Wang, W.; Wang, A.; Zhang, T. Discriminating Catalytically Active FeN_x Species of Atomically Dispersed Fe–N–C Catalyst for Selective Oxidation of the C–H Bond. *J. Am. Chem. Soc.* **2017**, *139*, 10790–10798.

(34) Jun, Y.; Park, J.; Lee, S. U.; Thomas, A.; Hong, W. H.; Stucky, G. D. From Melamine-Cyanuric Acid Supramolecular Aggregates to Carbon Nitride Hollow Spheres. *Angew. Chem., Int. Ed.* **2013**, *52*, 11083–11087.

(35) Niu, P.; Liu, G.; Cheng, H. Nitrogen Vacancy-Promoted Photocatalytic Activity of Graphitic Carbon Nitride. *J. Phys. Chem. C* **2012**, *116*, 11013–11018.

(36) Tay, Q.; Kanhere, P.; Ng, C. F.; Chen, S.; Chakraborty, S.; Huan, A. C. H.; Sum, T. C.; Ahuja, R.; Chen, Z. Defect Engineered g-C₃N₄ for Efficient Visible Light Photocatalytic Hydrogen Production. *Chem. Mater.* **2015**, *27*, 4930–4933.

(37) Ong, W.; Tan, L.; Ng, Y. H.; Yong, S.; Chai, S. Graphitic Carbon Nitride (g-C₃N₄)-Based Photocatalysts for Artificial Photosynthesis and Environmental Remediation: Are We a Step Closer To Achieving Sustainability. *Chem. Rev.* **2016**, *116*, 7159–7329.

(38) Chen, Z.; Zhang, Q.; Chen, W.; Dong, J.; Yao, H.; Zhang, X.; Tong, X.; Wang, D.; Peng, Q.; Chen, C.; He, W.; Li, Y. Single-Site Au^I Catalyst for Silane Oxidation with Water. *Adv. Mater.* **2018**, *30*, 1704720.

(39) Cheng, C.; Li, S.; Xia, Y.; Ma, L.; Nie, C.; Roth, C.; Thomas, A.; Haag, R. Atomic Fe–N_x Coupled Open-Mesoporous Carbon Nanofibers for Efficient and Bioadaptable Oxygen Electrode in Mg–Air Batteries. *Adv. Mater.* **2018**, *30*, 1802669.

(40) Wiles, A. B.; Bozzuto, D.; Cahill, C. L.; Pike, R. D. Copper (I) and (II) complexes of melamine. *Polyhedron* **2006**, *25*, 776–782.

(41) Li, F.; Han, G.; Noh, H.; Kim, S.; Lu, Y.; Jeong, H.; Fu, Z.; Baek, J. Boosting oxygen reduction catalysis with abundant copper single atom active sites. *Energy Environ. Sci.* **2018**, *11*, 2263–2269.

(42) Frenkel, A. I.; Wang, Q.; Marinkovic, N.; Chen, J.; Barrio, L.; Si, R.; Cámara, A. L.; Estrella, A. M.; Rodriguez, J. A.; Hanson, J. C. Combining X-ray Absorption and X-ray Diffraction Techniques for in Situ Studies of Chemical Transformations in Heterogeneous Catalysis: Advantages and Limitations. *J. Phys. Chem. C* **2011**, *115*, 17884–17890.

(43) Wang, D.; Wang, M.; Li, Z. Fe-Based Metal–Organic Frameworks for Highly Selective Photocatalytic Benzene Hydroxylation to Phenol. *ACS Catal.* **2015**, *5*, 6852–6857.

(44) Morimoto, Y.; Bunno, S.; Fujieda, N.; Sugimoto, H.; Itoh, S. Direct Hydroxylation of Benzene to Phenol Using Hydrogen Peroxide Catalyzed by Nickel Complexes Supported by Pyridylalkylamine Ligands. *J. Am. Chem. Soc.* **2015**, *137*, 5867–5870.